Enhancing Iterative Learning Control With Fractional Power Update Law

Zihan Li ⓘ, Dong Shen ⓘ, *Senior Member, IEEE*, and Xinghuo Yu ⓘ, *Fellow, IEEE*

Abstract—The P-type update law has been the mainstream technique used in iterative learning control (ILC) systems, which resembles linear feedback control with asymptotical convergence. In recent years, finite-time control strategies such as terminal sliding mode control have been shown to be effective in ramping up convergence speed by introducing fractional power with feedback. In this paper, we show that such mechanism can equally ramp up the learning speed in ILC systems. We first propose a fractional power update rule for ILC of single-input-single-output linear systems. A nonlinear error dynamics is constructed along the iteration axis to illustrate the evolutionary converging process. Using the nonlinear mapping approach, fast convergence towards the limit cycles of tracking errors inherently existing in ILC systems is proven. The limit cycles are shown to be tunable to determine the steady states. Numerical simulations are provided to verify the theoretical results.

Index Terms—Asymptotic convergence, convergence rate, finite-iteration tracking, fractional power learning rule, limit cycles.

I. INTRODUCTION

MOST production systems operate in a batch mode, where the plant repeatedly completes a given task in a finite-time interval. In such systems, traditional control methodologies based on the feedback principle fail to improve control performance from one batch to another. To effectively use the experience in previous batches, iterative learning control (ILC) has been proposed and has attracted substantial attention [1]. It improves control performance by refining the input signal based on tracking errors generated in previous batches, in addition to establishing an inherent feedback principle between successive batches for input generation and a connection between ILC and conventional control methodologies. Various theoretical issues have been comprehensively investigated, such as nonrepetitive uncertainties [2], data-driven methods [3], novel control structure [4], networked information communication [5], and stochastic learning control [6].

In the literature, two fundamental design paradigms have

been longstanding principal ideas of ILC. The first is the contraction mapping (CM) method based on the fixed point principle [7]–[9]. The tracking error is linearly added to the input, referred to as the P-type update law, such that a contraction is established for the input/output error along the batch axis. The other is the adaptive ILC (AILC) method associated with the Lyapunov function for analysis [10]–[12]. The system is linearly parameterized, and unknown parameters are iteratively estimated following the P-type update law. Asymptotic convergence of tracking errors is ensured generally as the batch number increases to infinity. However, the improving effect degrades as the error magnitude is reduced because of the linear learning structure in both paradigms. This is an outstanding issue and designing a novel paradigm with an accelerated convergence rate is of great interest and importance.

This observation motivates studies on finite-iteration convergence of ILC [13], [14]. However, it was limited to the exponentially decreasing trend of tracking error strongly related to the CM method. Further, it only guarantees finite-iteration convergence to a prior specified bounded zone rather than zero. In other words, the inherent convergence rate is not accelerated, especially at the later stage where the output has approached the neighbourhood of the desired reference. To solve this problem, one promising direction is to introduce a batch-varying gain sequence into the scheme [15]. However, the gain adaptation mechanisms are primarily for stochastic systems to address the noise effect.

It should be noted that the convergence behaviors of existing paradigms are generally unsatisfactory when tracking performance is required to reach a high level of precision. In particular, the constant and manually selected varying learning gains cannot assist in effectively utilizing the available information for update at this stage. This inspires us to look beyond the P-type update law in both paradigms, investigating a nonlinear update schema which may deliver superior performance.

In this paper, we propose a fractional power update rule to improve convergence speed, inspired by finite-time controllers (FTCs) [16]–[18] and terminal sliding mode control (TSMC) [19]–[21]. With continuous-time sliding model control, FTC can be realized by designing fractional power sliding manifolds, resulting in TSMC. Furthermore, many control laws have been designed to enable finite-time convergence by using the fractional-power Lyapunov function [22]–[24]. Note that finite-time convergence may be reduced to a bounded zone for discrete-time systems [25], [26]. Inspired by the

above results, we replace the linear update term in the P-type update rule by a fractional power term to accelerate the convergence rate.

We consider ILC of the single-input-single-output (SISO) time-invariant linear systems, which can be extended to the time-varying case. The update rule is built as a linear combination of the input and fractional-power tracking error of the previous iteration. This significantly differs from the traditional linear update in the CM and AILC methods. The proposed update rule follows a nonlinear update mode in essence, whereas the update mode is linear for both CM and AILC methods. Therefore, the analysis methods of CM and AILC are no longer applicable. We establish asymptotic convergence (Theorems 1–3) and depict limit cycles of the error dynamics (Theorem 4) for the novel update approach over the time interval using the nonlinear mapping approach. A nonlinear error dynamics is constructed in relation to the batch number and its evolution behavior is carefully investigated. The convergence is established by combining two key evolution properties, i.e., strict contraction between adjacent iterations for large tracking errors and locally asymptotical stability for small tracking errors. This analysis method includes the CM method as a special case. Numerical simulations are provided to demonstrate possible limit cycles and accelerated convergence performance.

To the best of our knowledge, this study is the first to investigate the use of fractional power in ILC as a new design paradigm. The contributions are threefold. First, the proposed algorithm follows a nonlinear update mode to provide more possibilities for extending learning ability. Second, the fractional power term can be regarded as a product of a regular error and an error-based varying gain. Thus, the convergence rate is adaptively regulated according to practical performance. Third, the fractional power update rule resembles fast convergence exhibited in FTC and TSMC. In addition, the conventional P-type update rule can be considered as a special case of the proposed update rule by letting the power be equivalent to one. The novelty of this study lies in the proposal of a fractional power update rule for ILC systems, nonlinear mapping-based convergence analysis method, and comprehensive characterization of limit cycles of tracking errors.

The remainder of this paper is organized as follows. Section II presents problem formulation and preliminaries. Section III addresses asymptotic convergence as the iteration number increases and depicts limit cycles. Section IV provides numerical simulations to verify the theoretical results. Section V concludes the paper.

Notations: We use $\lim_{k\to\infty} x_k = \pm x^*$ to denote that the sequence $\{x_k\}$ converges to a limit cycle consisting of x^* and $-x^*$. It is understood that as $\lim_{k\to\infty} x_{2k} = x^*$, $\lim_{k\to\infty} x_{2k+1} = -x^*$ or $\lim_{k\to\infty} x_{2k} = -x^*$, $\lim_{k\to\infty} x_{2k+1} = x^*$. $\rho(A)$ denotes the spectral radius of a matrix A. We use e_{ct} and e_{tc} to denote the limit of the error sequence at time instant t, where e_{ct} denotes the absolute value, and e_{tc} denotes its possible values, i.e., $e_{ct} = |e_{tc}|$.

II. PROBLEM FORMULATION

Consider the following SISO system:

$$x_k(t+1) = Ax_k(t) + bu_k(t)$$
$$y_k(t) = cx_k(t) \tag{1}$$

where $x_k(t) \in \mathbb{R}^m$, $u_k(t) \in \mathbb{R}$, and $y_k(t+1) \in \mathbb{R}$ are the state, input, and output, respectively. Matrices $A \in \mathbb{R}^{m\times m}$, $b \in \mathbb{R}^m$, and $c^T \in \mathbb{R}^m$ have appropriate dimensions. Furthermore, $t = 0, 1, \ldots, n$ and $k \in \mathbf{N}$ are the time and iteration labels, respectively, where n represents the iteration length.

Assumption 1: For each iteration, the initial state is reset to the same value, i.e., $x_{k+1}(0) = x_k(0)$, $\forall k$.

Assumption 1 is more relaxed than the well-known identical initialization condition (i.i.c.), which is widely used in the literature. In this study, we employ this assumption to simplify subsequent derivations and highlight our main innovations. Extensions to other variants of the initialization condition can be studied in future research.

For (1), we apply the fractional power update rule

$$u_{k+1}(t) = u_k(t) + \alpha|e_k(t+1)|^\gamma \text{sgn}(e_k(t+1)) \tag{2}$$

where α, $0 < \gamma < 1$, and $e_k(t)$ denotes the learning gain, fractional order, and tracking error, respectively. Here, $e_k(t) \triangleq y_d(t) - y_k(t)$ where $y_d(t)$ denotes the reference. Both α and γ are arbitrary constants. Throughout this article, we assume $\alpha cb > 0$. In addition, $\text{sgn}(\cdot)$ represents the sign function.

Remark 1: We compare (2) with the widely-used P-type update rule $u_{k+1}(t) = u_k(t) + \alpha e_k(t+1)$. We observe that the innovation term $e_k(t+1)$ in the P-type update rule is replaced by $|e_k(t+1)|^\gamma \text{sgn}(e_k(t+1))$ in (2). While the tracking error decreases to zero, $|e_k(t+1)|^\gamma \text{sgn}(e_k(t+1))$ would be larger than $|e_k(t+1)|$, implying that the update intensity of (2) will be stronger than the P-type update rule. This is an intuition for accelerating the convergence rate by the fractional power update rule (2). In addition, if we let γ be one, (2) becomes the P-type update rule, while if we let γ be zero, (2) becomes a bang-bang-like update rule [27]. In other words, the proposed update rule bridges the P-type and bang-bang-like update rules.

Denote $\delta x_k(t) = x_{k+1}(t) - x_k(t)$ and $\delta u_k(t) = u_{k+1}(t) - u_k(t)$ as the state- and input-difference of adjacent iterations. From (1), we present the iteration of the tracking error

$$
\begin{aligned}
e_{k+1}(t) &= e_k(t) - c\delta x_k(t) \\
&= e_k(t) - cA\delta x_k(t-1) - cb\delta u_k(t-1) \\
&= e_k(t) - \alpha cb|e_k(t)|^\gamma \text{sgn}(e_k(t)) - cA\delta x_k(t-1) \\
&= e_k(t) - \alpha cb|e_k(t)|^\gamma \text{sgn}(e_k(t)) \\
&\quad - \alpha \sum_{j=1}^{t-1} cA^j b|e_k(t-j)|^\gamma \text{sgn}(e_k(t-j)).
\end{aligned}
\tag{3}
$$

Control Objective: Our objective is to establish the convergence theory for the fractional power update rule (2) based on the error dynamics given by (3) in this study. In particular, we will prove the iteration-wise convergence and determine the convergence limit (cycles) for (2).

To facilitate the analysis, we first present several definitions and technical lemmas. The proofs for the lemmas are given in the appendix for readability.

Definition 1 (Limit cycle): For the sequence $\{x_k\}$, x_k is called

to converge to the limit cycle $\pm x_c$ if $|x_k| \to x_c$ and there exists K such that for any $k > K$, x_k and x_{k+1} have the opposite sign.

Definition 2: We have following definitions a) ~ f):

a) Given $f : \mathbb{R}^n \to \mathbb{R}^n$, define $f^i(u) \triangleq \underbrace{f(f(\cdots f(u)))}_{i}$;

b) For $u \in \mathbb{R}^n$ and $r > 0$, a ball with a center u and radius r is defined by $B(u, r) = \{v \in \mathbb{R}^n : \|v - u\| < r\}$;

c) Suppose v is the equilibrium of f, i.e., $f(v) = v$. If for $\forall \varepsilon > 0$, $\exists \delta > 0$, such that when $u \in B(v, \delta)$, $f^i(u) \in B(v, \varepsilon)$, $i = 1, 2, \ldots$, v is local stable;

d) If there exists a ball $B(v, r)$ such that $\lim_{i \to \infty} f^i(u) = v$ for every $u \in B(v, r)$, v is an attractor in $B(v, r)$;

e) If v is stable and locally attractive, v is locally asymptotically stable;

f) If $r = \infty$ in d) and v is stable, v is globally asymptotically stable.

Definition 3: Assume v is the equilibrium of f. Function $V : \mathbb{R}^n \to \mathbb{R}$ is continuous satisfying $V(v) = 0$ and for every $u \neq v$, $V(u) > 0$. If there exists a ball with a center v such that for any $u \in B$, $\Delta V(u) = V(f(u)) - V(u) \leq 0$, $V(x)$ is called a Lyapunov function of f at v. If $\forall u \neq v$ and $u \in B$, $\Delta V(u) < 0$, $V(x)$ is called a strict Lyapunov function.

Lemma 1 ([28]): Assume $v \in \mathbb{R}^n$ is the equilibrium of $f : \mathbb{R}^n \to \mathbb{R}^n$. Suppose there exists a ball with a center v such that f is continuous in the ball. If there exists a Lyapunov function of f at v, v is stable. If the Lyapunov function is strict, v is locally asymptotically stable.

Lemma 2: Assume v is the equilibrium of f and B is a ball with a center v. If $\|f(u) - v\| < \|u - v\|$, $\forall u \in B$, $v \neq u$, the iterative sequence generated by $u_{k+1} = f(u_k)$ with any initial value in B eventually converges to v.

Lemma 3: Consider an iterative sequence $x_{k+1} = f(x_k)$, where $f(x)$ is continuously differentiable. Assume x^* is the equilibrium and $|f'(x^*)| > 1$. For any initial value x_0, if there does not exist k satisfying $x_k = x^*$, we have $x_k \nrightarrow x^*$.

Then, we consider the case of nonlinear vector mapping as follows:

$$X(k + 1) = F(X(k)) \qquad (4)$$

where $X(k + 1) = [x_1(k), x_2(k), \ldots, x_n(k)]^T \in \mathbb{R}^n$ and

$$F(X(k)) = \begin{bmatrix} f_1(x_1(k), x_2(k), \ldots, x_n(k)) \\ f_2(x_1(k), x_2(k), \ldots, x_n(k)) \\ \vdots \\ f_n(x_1(k), x_2(k), \ldots, x_n(k)) \end{bmatrix}.$$

Define $\nabla f(x_1, x_2, \ldots, x_n) \triangleq [f_{x_1}, f_{x_2}, \ldots, f_{x_n}]^T$ and $\nabla F(X) \triangleq \left[\frac{\partial f_i}{\partial x_j} \right]_{n \times n}$.

Lemma 4: Suppose $X^* = [x_1^*, x_2^*, \ldots, x_n^*]^T$ is the equilibrium of (4), that is, $X^* = F(X^*)$. If $\rho(\nabla F(X^*)) < 1$, there exists a ball $B(X^*, r)$ with center X^* and radius r such that, for any $X(0) = X_0 \in B(X^*, r)$ as the initial value of (4), we have $\lim_{k \to \infty} X(k) = X^*$.

III. CONVERGENCE ANALYSIS OF FRACTIONAL POWER UPDATE RULE

In this section, we investigate the convergence of the frac-

tional power update rule (2) based on error dynamics (3). We analyze the rule following the induction principle with respect to the time label t. The case of $t = 1$ corresponds to a special case of the error dynamics (3) yielding a straightforward convergence analysis. For the case of $t = 2$, an additional disturbance term arises in the error dynamics, which complicates the analysis; however, the discussions of the following inductive cases are straightforward following this case. After that, the convergence limit cycles are summarized in Section III-D.

A. Case: $t = 1$

Let us start with the case of $t = 1$ for (3)

$$e_{k+1}(1) = e_k(1) - \alpha c b |e_k(1)|^\gamma \mathrm{sgn}(e_k(1)). \qquad (5)$$

We first clarify the limit (cycle) of (5) provided that it exists. In particular, we have two scenarios:

1) Assuming an equilibrium $e_e(1)$ exists, replacing $e_{k+1}(1)$ and $e_k(1)$ in (5) with $e_e(1)$ leads to $e_e(1) = 0$;

2) Assuming a limit cycle $\pm e_c(1)$ exists, replacing $e_{k+1}(1)$ and $e_k(1)$ in (5) with $e_c(1)$ and $-e_c(1)$, respectively, results in $e_c(1) = \frac{\alpha c b}{2} |e_c(1)|^\gamma \mathrm{sgn}(e_c(1))$; thus, $e_c(1) = (\frac{\alpha c b}{2})^{\frac{1}{1-\gamma}}$ if $e_c(1) > 0$ and $e_c(1) = -(\frac{\alpha c b}{2})^{\frac{1}{1-\gamma}}$ if $e_c(1) < 0$.

Then, we obtain the possible limits: an equilibrium $e_e(1) = 0$ and a limit cycle $e_c(1) = \pm \left(\frac{\alpha c b}{2} \right)^{\frac{1}{1-\gamma}}$.

Taking the absolute value for the both sides of (5), we have

$$|e_{k+1}(1)| = |e_k(1) - \alpha c b |e_k(1)|^\gamma \mathrm{sgn}(e_k(1))|$$
$$= |1 - \alpha c b |e_k(1)|^{\gamma - 1}| \cdot |e_k(1)|. \qquad (6)$$

When $|e_k(1)| \geq (\alpha c b)^{\frac{1}{1-\gamma}}$, $|e_{k+1}(1)| = \varphi(|e_k(1)|) \triangleq (1 - \alpha c b |e_k(1)|^{\gamma-1})|e_k(1)|$. We denote the set $\mathcal{A}^+ \triangleq \{a \geq 0 :$ there exists an integer i such that $\varphi^i(a) = 0\}$. The following lemma illustrates the convergence of $|e_k(1)|$.

Lemma 5: Suppose $|e_k(1)| > 0$ satisfies the difference equation (6). If $|e_0(1)| \in \mathcal{A}^+$, we obtain $|e_k(1)| = 0$ for $k \geq k_1$, where k_1 is a suitable number. If $|e_0(1)| \in [0, \infty) \backslash \mathcal{A}^+$, we have $\lim_{k \to \infty} |e_k(1)| = (\frac{\alpha c b}{2})^{\frac{1}{1-\gamma}}$.

Proof: If $|e_0(1)| \in \mathcal{A}^+$, $|e_k(1)| \equiv 0$ for $k \geq k_1$ where an integer k_1 exists. We consider the case $|e_0(1)| \in [0, \infty) \backslash \mathcal{A}^+$. The discussion is divided into two scenarios according to the range of the initial value $|e_0(1)|$.

Scenario A: $0 < |e_0(1)| < (\alpha c b)^{\frac{1}{1-\gamma}}$. We first prove that $0 < |e_{k+1}(1)| < (\alpha c b)^{\frac{1}{1-\gamma}}$ if $0 < |e_k(1)| < (\alpha c b)^{\frac{1}{1-\gamma}}$. Construct a function: $f(x) = |x - \alpha c b |x|^\gamma \mathrm{sgn}(x)|$. It is evident that $|e_{k+1}(1)| = f(|e_k(1)|)$. For any $0 < x < (\alpha c b)^{\frac{1}{1-\gamma}}$, we have $f(x) = \alpha c b x^\gamma - x$. Calculating $f'(x) = \gamma \alpha c b x^{\gamma-1} - 1 = 0$, we have $x = x_0 \triangleq (\gamma \alpha c b)^{\frac{1}{1-\gamma}} < (\alpha c b)^{\frac{1}{1-\gamma}}$. Then, for $x \in (0, x_0)$, $f'(x) > 0$ and $f(x)$ is monotonically increasing. Thus, when $|e_k(1)| \in (0, (\alpha c b)^{\frac{1}{1-\gamma}})$,

$$|e_{k+1}(1)| = f(|e_k(1)|) \leq f(x_0) = \gamma^{\frac{1}{1-\gamma}} (\frac{1}{\gamma} - 1)(\alpha c b)^{\frac{1}{1-\gamma}}$$
$$= \gamma^{\frac{\gamma}{1-\gamma}} (1 - \gamma)(\alpha c b)^{\frac{1}{1-\gamma}} < (\alpha c b)^{\frac{1}{1-\gamma}}.$$

That is, $|e_{k+1}(1)| \in (0, (\alpha c b)^{\frac{1}{1-\gamma}})$.

Define $e_{c1} \triangleq (\frac{\alpha c b}{2})^{\frac{1}{1-\gamma}}$, $e_r \triangleq (\alpha c b)^{\frac{1}{1-\gamma}}$. Next, we prove that for

every $|e_k(1)| \in (0, (\alpha cb)^{\frac{1}{1-\gamma}})$, $|e_k(1)| \neq e_{c1}$, we have $|f(|e_k(1)|) - e_{c1}| < ||e_k(1)| - e_{c1}|$. Because $\nabla^2 f = \gamma(\gamma-1)\alpha cbx^{\gamma-2} < 0$, $f(x)$ is a strictly concave function if $x \in (0, (\alpha cb)^{\frac{1}{1-\gamma}})$. Observing the graph of f in Fig. 1, we have $\left|\frac{f(x)-f(0)}{x}\right| \leq 1$ for any $0 \leq x \leq e_{c1}$ because e_{c1} is the intersection point of the line $y = x$ and curve $y = f(x)$. Moreover, $\left|\frac{f(e_r)-f(e_{c1})}{e_r-e_{c1}}\right| = \frac{(\frac{\alpha cb}{2})^{\frac{1}{1-\gamma}}}{(\alpha cb)^{\frac{1}{1-\gamma}}-(\frac{\alpha cb}{2})^{\frac{1}{1-\gamma}}} = \frac{1}{2^{\frac{1}{1-\gamma}}-1} < 1$. Therefore, for every $|e_k(1)| \in (0, (\alpha cb)^{\frac{1}{1-\gamma}})$, $|e_k(1)| \neq e_{c1}$, $\left|\frac{f(e_{c1})-f(|e_k(1)|)}{e_{c1}-|e_k(1)|}\right| < 1$; that is, $|f(e_{c1}) - f(|e_k(1)|)| < |e_{c1} - |e_k(1)||$.
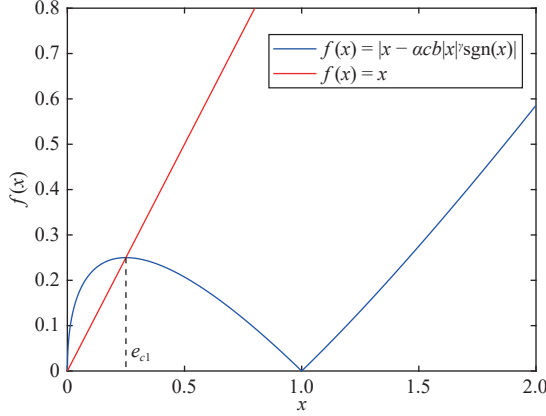

Fig. 1.　　Graph of $f(x) = |x - \alpha cb|x|^\gamma \text{sign}(x)|$ and $f(x) = x$ with $\alpha cb = 1$ and $\gamma = \frac{1}{2}$.

Because e_{c1} is the equilibrium of f, by Lemma 2, we obtain that $(\frac{\alpha cb}{2})^{\frac{1}{1-\gamma}}$ is asymptotically stable in $(0, (\alpha cb)^{\frac{1}{1-\gamma}})$. In other words, for every $0 < |e_0(1)| < (\alpha cb)^{\frac{1}{1-\gamma}}$, we can obtain $\lim_{k\to\infty}|e_k(1)| = (\frac{\alpha cb}{2})^{\frac{1}{1-\gamma}}$.

Scenario B: $|e_0(1)| > (\alpha cb)^{\frac{1}{1-\gamma}}$ and $|e_0(1)| \notin \mathcal{A}^+$. From (6), it follows $|e_k(1)| < (1 - \alpha cb|e_0(1)|^{\gamma-1})^k|e_0(1)| \to 0$. This demonstrates that there must exist a sufficiently large integer K such that $|e_k(1)| \in (0, (\alpha cb)^{\frac{1}{1-\gamma}})$, $\forall k > K$. This brings us back to Scenario A. ∎

Denote $\mathcal{A} \triangleq \{a : \text{either } a \in \mathcal{A}^+ \text{ or } -a \in \mathcal{A}^+\}$. It is clear that $\mathcal{A}$ consists of infinite discrete values. The following theorem is a corollary of Lemma 5.

Theorem 1: Consider the error dynamics (5). If $e_0(1) \in \mathcal{A}$, there exists k_1 such that $e_k(1) = 0$ for every $k \geq k_1$. If $e_0(1) \in [0, \infty)\backslash\mathcal{A}$, we obtain $\lim_{k\to\infty}|e_k(1)| = (\frac{\alpha cb}{2})^{\frac{1}{1-\gamma}}$, and when k is sufficiently large, $e_k(1)$ and $e_{k+1}(1)$ have opposite signs.

We merely need to demonstrate that $e_k(1)$ and $e_{k+1}(1)$ have opposite signs for a sufficiently large number of iterations. Based on Lemma 5, it is evident that $|e_k(1)| < (\alpha cb)^{\frac{1}{1-\gamma}}$ provided that $e_0(1) \notin \mathcal{A}$. Then, from the iteration $e_{k+1}(1) = (1 - \alpha cb|e_k(1)|^{\gamma-1})e_k(1)$, the conclusion is valid.

Theorem 1 illustrates that $e_k(1)$ converges to the limit cycle $\pm(\frac{\alpha cb}{2})^{\frac{1}{1-\gamma}}$ for most initial values (i.e., $e_0(1) \notin \mathcal{A}$). Next, we demonstrate the case of $e_k(2)$.

B. Case: $t = 2$

If the initial value $e_0(1) \in \mathcal{A}$, there exists k_1 such that $e_k(1) = 0$ for every $k \geq k_1$ (see Theorem 1). Then, the discussion for $t = 2$ degenerates to the case of $t = 1$ given in Section III-A. We consider the case $e_0(1) \notin \mathcal{A}$. The error dynamics (3) becomes

$$e_{k+1}(2) = e_k(2) - \alpha cb|e_k(2)|^\gamma \text{sgn}(e_k(2)) - \alpha cAb|e_k(1)|^\gamma \text{sgn}(e_k(1)). \tag{7}$$

As $k \to \infty$, $e_k(1)$ is approximately between $\pm(\frac{\alpha cb}{2})^{\frac{1}{1-\gamma}}$; thus, $e_k(2)$ cannot have any equilibrium. We denote the limit cycle $\pm e_{c2}$ of $e_k(2)$, assuming its existence. Then, we consider the following iteration to solve e_{c2}:

$$x_{k+1} = x_k - \alpha cb|x_k|^\gamma \text{sgn}(x_k) + (-1)^k M_1 \tag{8}$$

where $M_1 = |\alpha cAb|e_{c1}^\gamma$ and $e_{c1} = (\frac{\alpha cb}{2})^{\frac{1}{1-\gamma}}$. Define $f_1(x)$ and $f_2(x)$ as follows:

$$f_1(x_k) = x_k - \alpha cb|x_k|^\gamma \text{sgn}(x_k) + M_1$$
$$f_2(x_k) = x_k - \alpha cb|x_k|^\gamma \text{sgn}(x_k) - M_1.$$

It is evident that $f_1(-x) = -f_2(x)$ for any x. The image consisting of $f_1(x)$ and $f_2(x)$ is symmetric about the center of the origin, where the distance from the origin to the intersection between the function and the vertical axis is M_1. Thus, the convergence of iteration (8) is closely related to that of the iteration $x_{k+1} = -f_1(x_k) = f_2(-x_k)$ or $x_{k+1} = -f_2(x_k) = f_1(-x_k)$. That is, if the iteration $x_{k+1} = -f_1(x_k) = f_2(-x_k)$ converges to a limit τ, the iteration (8) converges to a limit cycle determined by the limit τ, and vice versa.

The limits for (8) are equivalent to the intersection of the two sets of curves below:

$$\text{curve group 1}: \begin{cases} y = -x + \alpha cb|x|^\gamma \text{sgn}(x) - M_1 \\ y = x \end{cases}$$

$$\text{curve group 2}: \begin{cases} y = -x + \alpha cb|x|^\gamma \text{sgn}(x) + M_1 \\ y = x. \end{cases}$$

Because the roots of *curve group 1* and *curve group 2* are opposite of each other, we only need to consider one of them. Let us consider the first curve group. To this end, we define an iteration as follows:

$$x_{k+1} = -x_k + \alpha cb|x_k|^\gamma \text{sgn}(x_k) - M_1 \triangleq g(x_k). \tag{9}$$

The solution of the first curve group corresponds to the limit of x_k generated by iteration (9) provided that the iteration is globally convergent, which will be shown below. Moreover, if (9) converges to x^*, the iteration (8) will converge to $\pm x^*$. In other words, the equilibrium of (9) corresponds to the limit cycle of (8). We investigate the convergence of (9), for which different values of M_1 will correspond to different scenarios. We discuss these different scenarios separately.

1) The first scenario corresponds to a large M_1. In this scenario, the two curves in *curve group 1* only intersect at one point, as depicted in Fig. 2(a). The intersection point is denoted by $P_1(a_1, a_1)$. Because P_1 is the intersection point of $y = x$ and $y = g(x)$, a_1 is the equilibrium of (9). Taking the derivative of the first curve in *curve group 1*, we obtain $y' = -1 + \gamma\alpha cb|x|^{\gamma-1}$ if $x \neq 0$ and $y' = \infty$ otherwise, indicating
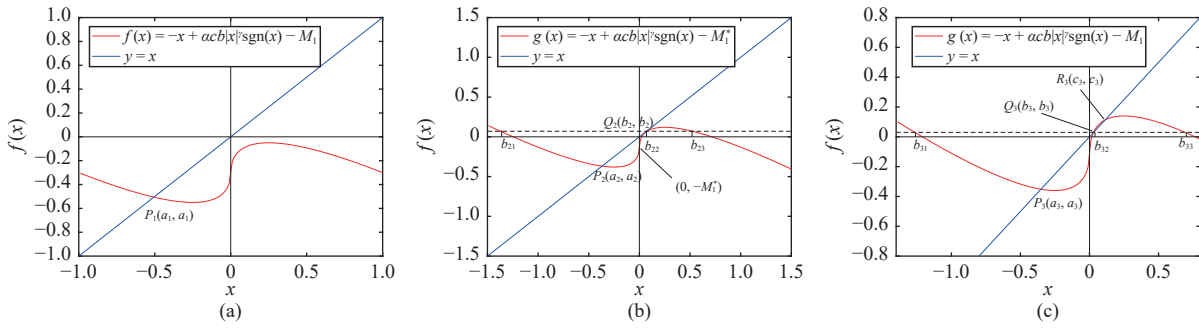
Fig. 2. (a) When M_1 is large, $y = -x + \alpha cb|x|^\gamma \mathrm{sgn}(x) - M_1$ and $y = x$ have only one intersection point $P_1(a_1, a_1)$; (b) The case that $y = -x + \alpha cb|x|^\gamma \mathrm{sgn}(x) - M_1$ and $y = x$ have two common points, where $P_2(a_2, a_2)$ is the intersection point and $Q_2(b_2, b_2)$ is the tangent point; (c) The case that $y = -x + \alpha cb|x|^\gamma \mathrm{sgn}(x) - M_1$ and $y = x$ have three intersection points: $P_3(a_3, a_3)$, $P_3(b_3, b_3)$, and $R_3(c_3, c_3)$.

that $\lim_{x \to \pm\infty} |g'(x)| = 1$. Thus, for any $u \in \mathbb{R}$ and $u \neq a_1$, we obtain $|g(u) - a_1| < |u - a_1|$. By Lemma 2, P_1 is globally asymptotically stable. Therefore, for any initial value x_0, x_k generated by (9) converges to a_1.

2) The second scenario corresponds to the situation where two curves are tangent at one point, as depicted in Fig. 2(b). In this scenario, the two curves have two intersecting points, denoted by $P_2(a_2, a_2)$ and $Q_2(b_2, b_2)$, where P_2 denotes a crossing point and Q_2 is a point of tangency. Because $-M_1 < 0$, we obtain $a_2 < 0$ and $b_2 > 0$. Observing the graph, by the increasing and decreasing trends of the function $g(x)$, the equation $g(x) = b_2$ has three roots, denoted by b_{21}, $b_{22}(= b_2)$, and b_{23} in Fig. 2(b), where $b_{21} < b_{22} < b_{23}$. We have the following propositions:

Proposition 1: For any $x \in [b_{22}, b_{23}]$, we obtain $g(x) \in [b_{22}, b_{23}]$. For any $x \in [b_{21}, b_{22}]$, we obtain $g(x) \in [b_{21}, b_{22}]$.

Proof: For $x > 0$, letting $g' = 0$, we obtain $x = \beta \triangleq (\gamma \alpha cb)^{\frac{1}{1-\gamma}}$. Because $b_{22} < \beta < b_{23}$, for any $x \in [b_{22}, b_{23}]$, we obtain $g(x) \geq g(b_{22}) = b_{22}$ and $g(x) \leq g(x_0) < \beta < b_{23}$. That is, $\forall x \in [b_{22}, b_{23}]$, $g(x) \in [b_{22}, b_{23}]$. In the same way, we can prove that $\forall x \in [b_{21}, b_{22}]$, $g(x) \in [b_{21}, b_{22}]$. ∎

Proposition 2: For any $x \in \mathbb{R} \setminus [b_{21}, b_{23}]$, we obtain $|g(x)| < |x|$. Thus, there is $0 < \rho(x) < 1$ such that $|g(x)| < \rho(x)|x|$.

Proof: According to the derivative expression of $g(x)$, there exists a constant M such that for any $|x| > M$, $|g'(x)| < 1$. Thus, the graph of $y = |g(x)|$ is strictly below the graph of $y = |x|$ when $x \in \mathbb{R} \setminus [b_{21}, b_{23}]$. ∎

For any $x \in (b_{21}, b_{22})$, $|g(x) - a_2| < |x - a_2|$; for any $x \in (b_{22}, b_{23})$, $|g(x) - b_2| < |x - b_2|$. According to Proposition 1 and Lemma 2, we obtain that a_2 is asymptotically stable in the interval $[b_{21}, b_{22}]$ and that b_2 is asymptotically stable in the interval $[b_{22}, b_{23}]$. According to Proposition 2, for any initial value $x_0 \in \mathbb{R}$, there must exist an integer $K(x_0)$, such that $x_k \in [b_{21}, b_{23}]$ for $k > K(x_0)$. Therefore, for any $x_0 \in \mathbb{R}$ and $x_{k+1} = g(x_k)$, it holds that either $x_k \to a_2$ or $x_k \to b_2$.

3) The third scenario corresponds to a small M_1. In this scenario, the two curves intersect at three points, as illustrated in Fig. 2(c). The intersecting points are denoted by $P_3(a_3, a_3)$, $Q_3(b_3, b_3)$, and $R_3(c_3, c_3)$ in ascending order. The equation $g(x) = b_3$ has three roots, denoted by b_{31}, $b_{32} = b_3$, and b_{33}. Besides, assume $b_{31} < b_{32} < b_{33}$. Similar to the second scenario, we obtain that for any $x \in [b_{31}, b_{32}]$, $g(x) \in [b_{31}, b_{32}]$, and for any $x \in [b_{32}, b_{33}]$, $g(x) \in [b_{32}, b_{33}]$. Moreover, for any

initial value $x_0 \in \mathbb{R}$, there must exist an integer $K(x_0)$ such that $x_k \in [b_{31}, b_{33}]$ for $k > K(x_0)$, where x_k is generated by (9). Combining this with Lemma 3, for any initial value x_0, we obtain the following conclusions:

A) If there exists x_{k_0} such that $x_{k_0} = b_3$, for any $k > k_0$, we obtain $x_k = b_3$;

B) If $x_k \neq b_3$, $\forall k \in \mathbf{N}$, either $x_k \to a_3$ or $x_k \to c_3$.

Thus far, we have discussed all the scenarios that can occur for the iteration (9) corresponding to *curve group 1*. Because $f_1(x)$ and $f_2(x)$ are symmetric about the origin, the results for *curve group 2* are exactly the same. In other words, the limit of the iteration $x_{k+1} = -x_k + \alpha cb|x_k|^\gamma \mathrm{sgn}(x_k) + M_1$ is similar to that of (9). The limit points of the former iteration and those of (9) are symmetric about the origin. Summarizing these results, we obtain the convergence of (8).

Remark 2: In the same way, we can show that for $t = 1$, the iteration $x_{k+1} = -x_k + \alpha cb|x_k|^\gamma \mathrm{sgn}(x_k)$ has the same convergence behavior as (5). Specifically, if the equilibrium of this iteration is e_{1c}, $\pm e_{1c}$ constitutes the limit cycle of (5).

Now, we go back to the convergence of the error iteration (7). When k is sufficiently large, $e_k(1)$ will vary between positive and negative values. From the previous discussions, (7) behaves the same as the iteration $e_{k+1}(2) = e_k(2) - \alpha cb|e_k(2)|^\gamma \mathrm{sgn}(e_k(2)) + (-1)^k \alpha cAb|e_k(1)|^\gamma$. We should emphasize that the convergence of (7) differs from that of (8) because the additional term (other than the main iteration variable) in (8) is a constant M_1, but it is iteration-varying in (7) because of $\alpha cAb|e_k(1)|^\gamma$.

We define $g_{1,k}(x) = x - \alpha cb|x|^\gamma \mathrm{sgn}(x) + |\alpha cAb| \cdot |e_k(1)|^\gamma$ and $g_{2,k}(x) = x - \alpha cb|x|^\gamma \mathrm{sgn}(x) - |\alpha cAb| \cdot |e_k(1)|^\gamma$. These two curves are symmetric about the origin. We demonstrate that (7) has the same convergence behavior as the iteration $e_{k+1}(2) = -g_{1,k}(e_k(2))$. That is, if $x^\star$ is a limit of $x_{k+1} = -g_{1,k}(x_k)$, $\pm|x^\star|$ constitutes the limit cycle of (7).

It has been proven that $e_k(1)$ converges to a limit cycle. Without loss of generality, we assume that $e_k(1) > 0$ for the odd iteration k and $e_k(1) < 0$ for the even iteration k. Then, the convergence of (7) is equivalent to the convergence of the following iteration:

$$x_{k+1} = \begin{cases} g_{1,k}(x_k), & k \text{ is an odd number} \\ g_{2,k}(x_k), & k \text{ is an even number.} \end{cases} \tag{10}$$

Lemma 6: If the iteration $x_{k+1} = g_{2,k}(-x_k)$ converges to a limit $x^\star$, (10) converges to a limit cycle $\pm|x^\star|$.

Proof: The proof is conducted in two steps. In the first step, we prove that when k is sufficiently large, the two adjacent iterations of (10) have opposite signs. In the second step, we prove the conclusion.

Step 1: Note that $\lim_{k \to \infty} |\alpha cAb| \cdot |e_k(1)|^\gamma = M_1$. For any $\varepsilon > 0$, we have $\||\alpha cAb| \cdot |e_k(1)|^\gamma - M_1| < \varepsilon$ when k is sufficiently large. Suppose x^* is the positive root of the equation $x - \alpha cbx^\gamma - (M_1 - \varepsilon) = 0$. Picking an arbitrary $x_k > 0$, we obtain the following two cases:

Case 1 (k is an even number): In this case, we have $x_{k+1} = x_k - \alpha cbx_k^\gamma - |\alpha cAb| \cdot |e_k(1)|^\gamma < x_k - \alpha cbx_k^\gamma - (M_1 - \varepsilon)$. We discuss the solution in two scenarios.

i) If $0 < x_k \leq x^*$, we obtain $x_{k+1} < 0$;

ii) For the scenario of $x^* < x_k$, if $x_{k+1} < 0$, x_k and x_{k+1} have opposite signs. Otherwise, if $x_{k+1} \geq 0$, we obtain

$$
\begin{aligned}
x_{k+2} &= x_{k+1} - \alpha cbx_{k+1}^\gamma + |\alpha cAb| \cdot |e_{k+1}(1)|^\gamma \\
&= x_k - \alpha cbx_k^\gamma - |\alpha cAb| \cdot |e_k(1)|^\gamma \\
&\quad - \alpha cbx_{k+1}^\gamma + |\alpha cAb| \cdot |e_{k+1}(1)|^\gamma \\
&\leq x_k - \alpha cbx_k^\gamma - \alpha cbx_{k+1}^\gamma + 2\varepsilon.
\end{aligned}
$$

Because $x_k > x^*$ and ε is a sufficiently small number, we obtain $x_{k+2} < x_k$. Thus, there must exist $k' > k$, which is an even number such that $0 < x_{k'} < x^*$ after which $x_{k'+1} < 0$.

Combining these two scenarios, for any $x_k > 0$, there must exist $k' \geq k$ such that $0 < x_{k'} < x^*$ and $x_{k'+1} < 0$. We now prove that $|x_k| < x^*$ is true for all $k > k'$ once $|x_{k'}| < x^*$. Without loss of generality, we suppose $0 < x_k < x^*$. Based on the above discussion, we obtain $x_{k+1} < 0$. Clearly, $-x^*$ is the negative root of $x - \alpha cb|x|^\gamma + (M_1 - \varepsilon) = 0$. Hence, we only need to prove $x_{k+1} > -x^*$. Denote $h(x) \triangleq x - \alpha cbx^\gamma - (M_1 + \varepsilon)$, where $h(x)$ takes the minimum value at $x = x_0 \triangleq (\gamma \alpha cb)^{\frac{1}{1-\gamma}}$ when $x > 0$. Hence, the minimum value of $h(x)$ for $x > 0$ is $h(x_0) = (1 - \frac{1}{\gamma})(\gamma \alpha cb)^{\frac{1}{1-\gamma}} - (M_1 + \varepsilon)$. We consider the root of $r(x) \triangleq x - \alpha cbx^\gamma - (M_1 - \varepsilon) = 0$. If the positive root of this equation is larger than $|h(x_0)|$, $x_{k+1} > -x^*$. Substituting $|h(x_0)|$ into the equation, we obtain

$$
\begin{aligned}
r(|h(x_0)|) &= |h(x_0)| - \alpha cb|h(x_0)|^\gamma - M_1 \\
&= \left(\frac{1}{\gamma} - 1\right)(\gamma \alpha cb)^{\frac{1}{1-\gamma}} \\
&\quad - \alpha cb\left[\left(\frac{1}{\gamma} - 1\right)(\gamma \alpha cb)^{\frac{1}{1-\gamma}} + M_1\right]^\gamma \\
&= \left\{\left(\frac{1}{\gamma} - 1\right) - \frac{1}{\gamma}\left[\left(\frac{1}{\gamma} - 1\right)\right.\right. \\
&\quad \left.\left. + (M_1 + \varepsilon)(\gamma \alpha cb)^{\frac{-1}{1-\gamma}}\right]^\gamma\right\}(\gamma \alpha cb)^{\frac{1}{1-\gamma}} + 2\varepsilon \\
&\leq \left[\left(\frac{1}{\gamma} - 1\right) - \frac{1}{\gamma}\left(\frac{1}{\gamma} - 1\right)^\gamma\right](\gamma \alpha cb)^{\frac{1}{1-\gamma}} + 2\varepsilon.
\end{aligned}
$$

If $\frac{1}{2} \leq \gamma < 1$, we have $\frac{1}{\gamma}(\frac{1}{\gamma} - 1)^\gamma > (\frac{1}{\gamma} - 1)$. If $0 < \gamma < \frac{1}{2}$, we have $\frac{1}{\gamma}(\frac{1}{\gamma} - 1)^\gamma > (\frac{1}{\gamma} - 1)^{\gamma+1} > (\frac{1}{\gamma} - 1)$. Therefore, for a sufficiently small ε, we obtain $r(|h(x_0)|) < 0$ and $x_{k+1} > -x^*$. Using the same method, we can prove $x_{k+2} < x^*$. Thus, x_k and x_{k+1} have the opposite signs for sufficiently large k.

Case 2 (k is an odd number): This scenario corresponds to a small value of M_1. Then, $\lim_{k \to \infty} g_{1,k}(x) = 0$ has two different positive roots. Using similar analysis to Case 1, we obtain that x_k and x_{k+1} have opposite signs for sufficiently large k. In addition, we obtain $0 < \xi_1 < |x_k| < \xi_2 < x_*$, where x_* represents the largest root of the equation $x - \alpha cb|x|^\gamma + (M + \varepsilon) = 0$, ε is a sufficiently small positive number, and ξ_1 and ξ_2 are two positive constants.

Step 2: Based on *Step 1*, for Case 1 with sufficiently large k, we rewrite (10) as

$$
x_{k+1} = \begin{cases} x_k - \alpha cb|x_k|^\gamma \text{sgn}(x_k) + |\alpha cAb| \cdot |e_k(1)|^\gamma, & x_k < 0 \\ x_k - \alpha cb|x_k|^\gamma \text{sgn}(x_k) - |\alpha cAb| \cdot |e_k(1)|^\gamma, & x_k \geq 0. \end{cases}
$$

Because x_{k+1} and x_k have opposite signs, taking absolute values of both sides, we obtain

$$
|x_{k+1}| = -|x_k| + \alpha cb|x_k|^\gamma + |\alpha cAb| \cdot |e_k(1)|^\gamma. \tag{11}
$$

Similarly, for Case 2 with sufficiently large k, we obtain

$$
|x_{k+1}| = -|x_k| + \alpha cb|x_k|^\gamma - |\alpha cAb| \cdot |e_k(1)|^\gamma \tag{12}
$$

where $\xi_1 < |x_k| < \xi_2$. The equilibriums of (11) and (12) are same to that of $x_{k+1} = g_{2,k}(-x_k)$. The image of (12) is identical to that of $x_{k+1} = g_{2,k}(-x_k)$ for $x_k > 0$, whereas the image of (11) is symmetric with that of $x_{k+1} = g_{2,k}(-x_k)$ about the origin for $x_k < 0$. ∎

Noticing that $e_k(1)$ converges to a limit cycle, the convergence of $e_{k+1}(2) = g_{2,k}(-e_k(2))$ is equivalent to that of (13).

$$
\begin{aligned}
\begin{bmatrix} e_{k+1}(1) \\ e_{k+1}(2) \end{bmatrix} &= G_2\left(\begin{bmatrix} e_k(1) \\ e_k(2) \end{bmatrix}\right) \\
&= \begin{bmatrix} -e_k(1) + \alpha cb|e_k(1)|^\gamma \text{sgn}(e_k(1)) \\ -e_k(2) + \alpha cb|e_k(2)|^\gamma \text{sgn}(e_k(2)) - |\alpha cAb| \cdot |e_k(1)|^\gamma \end{bmatrix}
\end{aligned} \tag{13}
$$

$$
\begin{aligned}
&G_2\left(\begin{bmatrix} e_k(1) \\ e_k(2) \end{bmatrix}\right) - \begin{bmatrix} e_{1c} \\ e_{2c} \end{bmatrix} \\
&= \begin{bmatrix} -e_k(1) + \alpha cb|e_k(1)|^\gamma \text{sgn}(e_k(1)) - e_{1c} \\ -e_k(2) + \alpha cb|e_k(2)|^\gamma \text{sgn}(e_k(2)) - |\alpha cAb| \cdot |e_k(1)|^\gamma - e_{2c} \end{bmatrix} \\
&= \begin{bmatrix} -e_k(1) + \alpha cb|e_k(1)|^\gamma \text{sgn}(e_k(1)) - e_{1c} \\ -e_k(2) + \alpha cb|e_k(2)|^\gamma \text{sgn}(e_k(2)) - M_1 - e_{2c} \end{bmatrix} \\
&\quad + \begin{bmatrix} 0 \\ M_1 - |\alpha cAb| \cdot |e_k(1)|^\gamma \end{bmatrix}.
\end{aligned} \tag{14}
$$

Note that

$$
\nabla G_2 = \begin{bmatrix} \gamma \alpha cb|e_k(1)|^{\gamma-1} - 1 & 0 \\ -\gamma \alpha cAb|e_k(1)|^{\gamma-1} & \gamma \alpha cb|e_k(2)|^{\gamma-1} - 1 \end{bmatrix}. \tag{15}
$$

For the limit cycle, we obtain

$$
\nabla G_2\left(\begin{bmatrix} e_{1c} \\ e_{2c} \end{bmatrix}\right) = \begin{bmatrix} \gamma \alpha cb|e_{1c}|^{\gamma-1} - 1 & 0 \\ -\gamma \alpha cAb|e_{1c}|^{\gamma-1} & \gamma \alpha cb|e_{2c}|^{\gamma-1} - 1 \end{bmatrix}.
$$

Here, e_{2c} is a solution of *curve group 1* (it may contain more than one value, which can be positive or negative), i.e., $\pm e_{2c}$ is the limit cycle of (8). Note that e_{tc} has an indeterminate sign, whereas e_{ct} denotes its absolute value, i.e., $e_{ct} = |e_{tc}|$. From (13), we obtain (14), where M_1 is given in (8). From

(14), convergence of $e_k(2)$ has no influence on $e_k(1)$. Define

$$G_{2k} \triangleq G_2\left(\begin{bmatrix} e_k(1) \\ e_k(2) \end{bmatrix}\right), E_{2k} \triangleq \begin{bmatrix} e_k(1) \\ e_k(2) \end{bmatrix}, E_{2c} \triangleq \begin{bmatrix} e_{1c} \\ e_{2c} \end{bmatrix}$$

$$E_{2k}^{M_1} \triangleq \begin{bmatrix} -e_k(1)+\alpha cb|e_k(1)|^{\gamma}\mathrm{sgn}(e_k(1))-e_{1c} \\ -e_k(2)+\alpha cb|e_k(2)|^{\gamma}\mathrm{sgn}(e_k(2))-M_1-e_{2c} \end{bmatrix}$$

$$\widetilde{E}_{2k}^{M_1} \triangleq \begin{bmatrix} 0 \\ M_1-|\alpha cAb|\cdot|e_k(1)|^{\gamma} \end{bmatrix}.$$

Then, for iteration (13), we have the following analysis.

Scenario A: Consider that (9) has one equilibrium e_{2c}. Based on the discussion of (9), we know $\rho(\nabla G_2(E_{2c})) < 1$, where $\rho(A)$ denotes the spectral radius of a matrix A. Thus, there must exist a neighborhood of (e_{1c}, e_{2c}), denoted by $U((e_{1c}, e_{2c}); r_1)$ with r_1 being the radius, such that $\rho(\nabla G_2(x)) < 1$, $\forall x \in U((e_{1c}, e_{2c}); r_1)$. As $k \to \infty$, the second entry of the matrix $\widetilde{E}_{2k}^{M_1} \to 0$. We select K_{11} such that $|e_{1c} - e_k(1)| < \varepsilon_0$ for a fixed $\varepsilon_0 < r_1$, $\forall k > K_{11}$.

Based on the analysis of (9), when the *curve group 1* has only one intersecting point, for any $e_k(2) \neq e_{2c}$, $|g(e_k(2)) - e_{2c}| < |e_k(2) - e_{2c}|$. Thus, there exists $\epsilon > 0$ such that for any $e_k(2) \in \mathbb{R} \setminus (e_{2c} - (r_1 - \varepsilon_0), e_{2c} + (r_1 - \varepsilon_0))$, we obtain $|-e_k(2) + \alpha cb|e_k(2)|^{\gamma}\mathrm{sgn}(e_k(2)) - M_1 - e_{2c}| = |g(e_k(2)) - e_{2c}| < |e_k(2) - e_{2c}| - \epsilon$. Because $|\alpha cAb||e_k(1)|^{\gamma} \to M_1$, we can select K_{12} such that $|M - |\alpha cAb||e_k(1)|^{\gamma}| < \varepsilon < \epsilon$, $\forall k > K_{12}$. Define $K_1 = \max\{K_{11}, K_{12}\}$. When $k > K_1$, for any $e_k(2) \in \mathbb{R} \setminus (e_{2c} - (r_1 - \varepsilon_0), e_{2c} + (r_1 - \varepsilon_0))$, we obtain $|-e_k(2) + \alpha cb|e_k(2)|^{\gamma}\mathrm{sgn}(e_k(2)) - M_1 - e_{2c}| + |M_1 - |\alpha cAb||e_k(1)|^{\gamma}| < |e_k(2) - e_{2c}| - \epsilon + \varepsilon < |e_k(2) - e_{2c}|$. Moreover, noticing that $|-e_k(1) + \alpha cb|e_k(1)|^{\gamma}\mathrm{sgn}(e_k(1)) - e_{1c}| < |e_k(1) - e_{1c}|$, we obtain that, for any $e_k(2) \in \mathbb{R} \setminus [e_{2c} - (r_1 - \varepsilon_0), e_{2c} + (r_1 - \varepsilon_0)]$,

$$\|G_2(E_{2k}) - E_{2c}\| = \|E_{2k}^{M_1} + \widetilde{E}_{2k}^{M_1}\| < \|E_{2k} - E_{2c}\|. \tag{16}$$

Here, the vector norm can be 1-, 2-, and ∞-norm as we have shown that the absolute value for each dimension of the vector decreases as iteration number increases.

Furthermore, for all $k > K_1$ and $e_k(2) \in (e_{2c} - (r_1 - \varepsilon_0), e_{2c} + (r_1 - \varepsilon_0))$, we obtain $(e_k(1), e_k(2)) \in U((e_{1c}, e_{2c}); r_1)$ and thus $\rho(\nabla G_2) < 1$. By Lemma 4, we obtain $\|G_2(E_{2k}) - E_{2c}\| < \|E_{2k} - E_{2c}\|$.

Combining the above two cases, for any $E_{2k} \in \mathbb{R}^2$, we obtain $\|G_2(E_{2k}) - E_{2c}\| < \|E_{2k} - E_{2c}\|$, $\forall k > K_1$. Because E_{2c} is the equilibrium of $G_2(\cdot)$, by Lemma 2, E_{2c} is globally asymptotically stable.

Scenario B: (9) has two equilibriums a_2 and b_2. We prove that either $E_{2k} \to [e_{1c}, a_2]^T$ or $E_{2k} \to [e_{1c}, b_2]^T$, where a_2 and b_2 represent the abscissae of the intersection and tangent points in Fig. 2(b), respectively. We obtain $\rho(\nabla G_2(E_{2c})) < 1$ with $e_{2c} = a_2$ and $\rho(\nabla G_2(E_{2c})) = 1$ with $e_{2c} = b_2$. For the latter case, we obtain $\frac{\partial^2 g_2(x,y)}{\partial y^2}|_{y=b_2} = \gamma(\gamma-1)\alpha cb|b_2|^{\gamma} < 0$, where $g_2(x,y) \triangleq -y + \alpha cb|y|^{\gamma}\mathrm{sgn}(y) - |\alpha cAb| \cdot |x|^{\gamma}$.

Similar to *Scenario A*, there exists K_{21} such that for any $k > K_{21}$, $|e_{k+1}(2) - a_2| < |e_k(2) - a_2|$, $\forall e_k(2) \in \mathbb{R} \setminus (a_2 - \varepsilon_0, b_2 + \varepsilon_0)$. Therefore, for $k > K_{21}$, any $e_k(2)$ outside the interval $(a_2 - \varepsilon_0, b_2 + \varepsilon_0)$ will enter it after finite iterations. We denote $k_1 \triangleq \min\{k \in \mathbf{N} \mid e_k(2) \in (a_2 - \varepsilon_0, b_2 + \varepsilon_0)\}$. Then, we have the

followings.

a) If $e_{k_1}(2) \in (a_2 - \varepsilon_0, b_2 - \varepsilon_0)$, by a similar analysis of *Scenario A*, we obtain that $e_k(2)$ converges to a_2;

b) If $e_{k_1}(2) \in (b_2 - \varepsilon_0, b_2 + \varepsilon_0)$, we have two subcases. If $E_{2k} \to [e_{1c}, b_2]^T$, the conclusion has been proved; otherwise, we consider the subcase that $E_{2k} \nrightarrow [e_{1c}, b_2]^T$ and prove that the limit is $[e_{1c}, a_2]^T$. Because $e_k(2) \nrightarrow b_2$, there exists ε_1 such that for any $K > 0$, there exists $k > K$ such that $|e_k(2) - b_2| > \varepsilon_1$. Considering the arbitrariness of ε_0 for determining the ball around a_2, we choose a constant $\varepsilon_0 < \varepsilon_1$. Because $e_k(1) \to e_{1c}$, there exists a sufficiently large K_{22} such that $||\alpha cAb|e_k(1)|^{\gamma} - \alpha cAb|e_{1c}|^{\gamma}| < \varepsilon_1 - \varepsilon_0$, $\forall k > K_{22}$. Now, we let $K_2 = \max\{K_{21}, K_{22}\}$. It is evident that for any $K > K_2$, there exists $k > K$ such that $|e_k(2) - b_2| > \varepsilon_1$. Therefore, if we can prove that $e_k(2)$ cannot be greater than $b_2 + \varepsilon_1$ for all $k > K_2$, it must be less than $b_2 - \varepsilon_1$, implying $e_k(2) < b_2 - \varepsilon_0$, which is convergent to a_2. This claim is illustrated by Fig. 3.
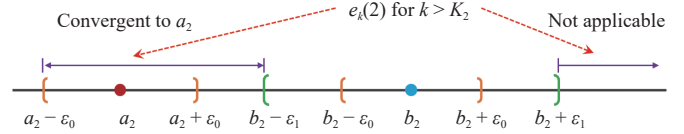

Fig. 3. Illustration of possible $e_k(2)$ after sufficiently many iterations.

We prove the claim now. Assume that $e_k(2) > b_2 + \varepsilon_1$. Similar to the definition of k_1, we know that after a sufficient number of iterations, say k_2, the tracking error is drawn back to the interval $(a_2 - \varepsilon_0, b_2 + \varepsilon_0)$. That is, $e_{k+k_2}(2) < b_2 + \varepsilon_0$, where $k > K_2$. We will demonstrate that the tracking error will be unable to exceed $b_2 + \varepsilon_1$ anymore. Noticing the fact of $\frac{\partial^2 g_2(x,y)}{\partial y^2}|_{y \geq b_2} < 0$, we obtain that $e_{k+1}(2) < b_2 + \varepsilon_0 + (\varepsilon_1 - \varepsilon_0) = b_2 + \varepsilon_1$ for any $k > K_2 + k_2$. This implies that $(b_2 + \varepsilon_1, \infty)$ is not a feasible interval for the tracking error $e_k(2)$. Thus, if $e_k(2)$ does not converge to b_2, it must be less than $b_2 - \varepsilon_1$ after a finite number of iterations.

Combining the two subcases, we can conclude that, for any initial value, either $\lim_{k \to \infty}[e_k(1), e_k(2)]^T = [e_{1c}, a_2]^T$ or $\lim_{k \to \infty}[e_k(1), e_k(2)]^T = [e_{1c}, b_2]^T$ holds.

Scenario C: (9) has three equilibriums a_3, b_3, and c_3 (see Fig. 2(c)). We obtain $\rho(\nabla G_2(E_{2c})) < 1$ with $e_{2c} = a_3$ and $e_{2c} = c_3$, and $\rho(\nabla G_2(E_{2c})) > 1$ if $e_{2c} = b_3$. For the latter case, there exists a neighborhood of (e_{1c}, b_3), denoted by $U((e_{1c}, b_3); r_2)$ with r_2 being the radius, such that for every $x \in U((e_{1c}, b_3); r_2)$, we obtain $\rho(\nabla G_2(x)) > 1$. Similar to the previous two scenarios, we can prove that there exists K_3 and ε_0 such that for $k > K_3$ and $e_k(2) \in (b_3 - (r_3 - \varepsilon_0), b_3 + (r_3 - \varepsilon_0))$, $\rho(\nabla G_2(E_{2k})) > 1$. Therefore, $e_k(2)$ will jump out of the interval after a finite number of iterations. Similar to *Scenario B*, we can prove that $[e_k(1), e_k(2)]^T$ will converge to either $[e_{1c}, a_3]^T$ or $[e_{2c}, c_3]^T$.

By combining these scenarios, the convergence of the iteration (13) has been proved. From Lemma 6, the convergence of $e_k(2)$ generated by (10) can be obtained. Because of the equivalence between (10) and (7), the convergence of (7) is obtained. It is summarized in the following theorem.

Theorem 2: Consider error dynamics (3) for $t = 2$ with the

initial error $(e_0(1), e_0(2))$. If $e_0(1) \in \mathcal{A}$, there exists k_2 such that $e_k(1) = 0$ for $k \geq k_2$ and $\lim_{k \to \infty} e_k(2) = \pm e_{1c}$. Otherwise, $\lim_{k \to \infty} e_k(1) = \pm e_{1c}$ and $\lim_{k \to \infty} e_k(2) = \pm e_{2c}$. Here, $|e_{1c}| = (\frac{\alpha cb}{2})^{\frac{1}{1-\gamma}}$, and e_{2c} is one root of the equation

$$x = -x + \alpha cb|x|^\gamma \text{sgn}(x) - M_1 \qquad (17)$$

with $M_1 = |\alpha cAb||e_{1c}|^\gamma$.

Remark 3: For different initial values of $e_0(1)$ and $e_0(2)$, $|e_k(2)|$ converges to different roots of (17). However, once $e_0(1)$ and $e_0(2)$ are determined, the limit of $|e_k(2)|$ is determined. Moreover, there exists a sufficiently large integer K_0 such that the value of $e_k(2)$ is approximately between $\pm e_{2c}$ for all $k > K_0$. Thus, $e_k(2)$ and $e_{k+1}(2)$ have opposite signs.

Theorem 2 demonstrates the convergence of $e_k(2)$. The specific limit is straightforward following the analysis procedure. In particular, we have the following results.

1) If $e_0(1) \in \mathcal{A}$, the evolution of $e_k(2)$ degenerates to the case of $t = 1$. That is, the convergence of $e_k(2)$ is the same as that of $e_k(1)$;

2) If $e_0(1) \notin \mathcal{A}$, the tracking error $e_k(2)$ converges to a limit cycle. The limit cycle is influenced by e_{1c}. Three possible scenarios have been illustrated in Fig. 2. Considering the special case of Fig. 2(b), where the curves are tangent, we calculate $M^* = 2(\frac{1}{\gamma} - 1)(\frac{\gamma \alpha cb}{2})^{\frac{1}{1-\gamma}}$, as shown in Fig. 2(b). Define a nonlinear equation by

$$x = -x + \alpha cb|x|^\gamma \text{sgn}(x) - |\alpha cAb||e_{1c}|^{\frac{\gamma}{1-\gamma}}. \qquad (18)$$

The convergence limits are clarified as follows.

a) If $|\alpha cAb||e_{1c}|^\gamma > M^*$, (18) has only one root, denoted by a_{11}. We obtain the limit cycle $\lim_{k \to \infty} e_k(2) = \pm|a_{11}|$ and $e_{c2} = |a_{11}|$;

b) If $|\alpha cAb||e_{1c}|^\gamma = M^*$, (18) has two roots a_{12} and b_{12}. We obtain the limit cycles $\lim_{k \to \infty} e_k(2) = \pm|a_{12}|$ and $\lim_{k \to \infty} e_k(2) = \pm|b_{12}|$. Moreover, $e_{c2} = |a_{12}|$ or $|b_{12}|$;

c) If $|\alpha cAb||e_{1c}|^\gamma < M^*$, (18) has three roots a_{13}, b_{13}, and c_{13}. Suppose $a_{13} < b_{13} < c_{13}$. Then, we obtain the limit cycles $\lim_{k \to \infty} e_k(2) = \pm|a_{13}|$ and $\lim_{k \to \infty} e_k(2) = \pm|c_{13}|$. Moreover, $e_{c2} = |a_{13}|$ or $|c_{13}|$.

Remark 4: In the latter two scenarios, two possible limit cycles exist. The final limit cycle depends on the initial value of (8), where $M_1 = |\alpha cAb||e_{1c}|^\gamma$. However, the actual iteration of $e_k(2)$ is conducted by (7), where the additional term $\alpha cAb|e_k(1)|^\gamma \text{sgn}(e_k(1))$ is not equal to M_1 but simply approaches M_1. Therefore, it is difficult to present the explicit range of the initial values for a given limit cycle.

C. Case: $t = n$

When $t = n$, from (3), we obtain

$$e_{k+1}(n) = e_k(n) - \alpha cb|e_k(n)|^\gamma \text{sgn}(e_k(n))$$
$$- \alpha \sum_{j=1}^{n-1} cA^j b|e_k(n-j)|^\gamma \text{sgn}(e_k(n-j)).$$

Following the induction principle, $\lim_{k \to \infty} e_k(t) = e_{tc}$ for $t \leq n - 1$, where e_{tc} can be a limit or limit cycle. For every $t > 1$, e_{tc} has multiple possible values; however, once the initial value is given, the limit (cycle) e_{tc} is determined. The conclusion for the case of $t = n$ is similar to the case of $t = 2$,

because the major difference lies in the replacement of $\alpha cAb|e_k(1)|^\gamma \text{sgn}(e_k(1))$ with $\alpha \sum_{j=1}^{n-1} cA^j b|e_k(n-j)|^\gamma \text{sgn}(e_k(n-j))$.

The following theorem shows the convergence of $e_k(t)$.

Theorem 3: Consider error dynamics (3) with initial values $[e_0(1), e_0(2), \ldots, e_0(n)]^T$. $[e_k(1), e_k(2), \ldots, e_k(n)]^T$ will converge to a nonzero limit cycle, and there exists K such that $e_k(i)$ and $e_{k+1}(i)$ have the opposite signs for $k > K$, $\forall i$.

Proof: In Sections III-A and III-B, we have shown the convergence for $t = 1$ and $t = 2$. Assuming that $e_k(t)$ is convergent for $t \leq n - 1$, i.e., $\lim_{k \to \infty} e_k(t) = \pm e_{tc}$, $\forall t \leq n - 1$, we define $M_{i-1}^k \triangleq \alpha \sum_{j=1}^{i-1} cA^j b|e_k(i-j)|^\gamma \text{sgn}(e_k(i-j))$ and $M_{i-1} \triangleq \lim_{k \to \infty} |M_{i-1}^k|$. Using these notations, we obtain (19). We first examine the equilibrium or limit cycle of this equation and then analyze asymptotic convergence in the iteration domain.

$$G_n\left(\begin{bmatrix} e_k(1) \\ e_k(2) \\ \vdots \\ e_k(n) \end{bmatrix}\right)$$

$$= \begin{bmatrix} -e_k(1) + \alpha cb|e_k(1)|^\gamma \text{sgn}(e_k(1)) \\ -e_k(2) + \alpha cb|e_k(2)|^\gamma \text{sgn}(e_k(2)) - |M_1^k| \\ \vdots \\ -e_k(n-1) + \alpha cb|e_k(n-1)|^\gamma \text{sgn}(e_k(n-1)) - |M_{n-1}^k| \end{bmatrix}$$
$$(19)$$

$$\nabla G_n\left(\begin{bmatrix} e_{1c} \\ e_{2c} \\ e_{3c} \\ \vdots \\ e_{nc} \end{bmatrix}\right) = \begin{bmatrix} \gamma \alpha cb|e_{1c}|^{\gamma-1} - 1 & 0 \\ -\gamma \alpha cAb|e_{1c}|^{\gamma-1} & \gamma \alpha cb|e_{2c}|^{\gamma-1} - 1 \\ -\gamma \alpha cA^2 b|e_{1c}|^{\gamma-1} & -\gamma \alpha cAb|e_{2c}|^{\gamma-1} \\ \vdots & \vdots \\ -\gamma \alpha cA^{n-1} b|e_{1c}|^{\gamma-1} & -\gamma \alpha cA^{n-2} b|e_{2c}|^{\gamma-1} \end{bmatrix}$$
$$\begin{matrix} 0 & \cdots & 0 \\ 0 & \cdots & 0 \\ \gamma \alpha cb|e_{3c}|^{\gamma-1} - 1 & \cdots & 0 \\ \vdots & \ddots & \vdots \\ -\gamma \alpha cA^{n-3} b|e_{3c}|^{\gamma-1} & \cdots & \gamma \alpha cb|e_{nc}|^{\gamma-1} - 1 \end{matrix} \Bigg].$$
$$(20)$$

Suppose $[e_{1c}, e_{2c}, \ldots, e_{nc}]^T$ is the equilibrium of (19), after which we obtain (20). In the same way that the case of $t = 2$ is analyzed, three scenarios of (21) can be examined,

$$x = -x + \alpha cb|x|^\gamma \text{sgn}(x) - M_{n-1} \qquad (21)$$

where $M_{n-1} = |\alpha \sum_{j=1}^{n-1} cA^j b|e_{(n-j)c}|^\gamma \text{sgn}(e_{(n-j)c})|$. In particular, the three scenarios correspond to cases that (21) has one, two, and three equilibriums similar to the analysis of (9). Given the initial value $[e_0(1), e_0(2), \ldots, e_0(n)]^T$, we obtain $\lim_{k \to \infty} e_k(n) = \pm e_{nc}$ for (19). Therefore, given any initial values $[e_0(1), e_0(2), \ldots, e_0(n)]^T$, we obtain $\lim_{k \to \infty} [e_k(1), e_k(2), \ldots, e_k(n)]^T = \pm[e_{1c}, e_{2c}, \ldots, e_{nc}]^T$. ∎

Remark 5: For the vector function (19), the analysis of each

entry is the same as that for (13). In particular, for the ith entry, all possible values of its limit cycle are calculated without considering their signs. In other words, the signs of the variables are indeterminate. For example, for a given group of initial errors, we may obtain the limit $e_{ic} = 0.5$ for the ith time instant by solving $G_n(\mathbf{x}) = \mathbf{x}$. Then, the actual limit cycle is ± 0.5. However, the signs are excluded from the diagonal elements of (20); therefore, the convergence is not influenced by the specific signs.

Remark 6: Different initial errors lead to different limit cycles. In (20), the notation of limits e_{ic} indicates any group of the limit cycles and (20) denotes its gradient. However, we have proven that the conclusion is valid for any possible candidate of the limit cycles.

D. Convergence Limit Cycles

In this subsection, we present the limit (cycle) of $e_k(t)$ by summarizing results in the previous subsections.

Denoting the absolute limit values of the errors at time instants $1 \le t \le n-1$ to be e_{ct}, we establish a nonlinear equation

$$-x = x - \alpha cb|x|^\gamma \text{sgn}(x) - \left| \alpha \sum_{j=1}^{n-1} (-1)^{\omega_j} cA^j be_{c(n-j)}^\gamma \right|$$

where $\omega_j \in \{0, 1\}$. Each combination of $\{\omega_1, \omega_2, \ldots, \omega_{n-1}\}$ corresponds to a certain case of the limit cycle generation. Denote $M_{n-1}^\omega = \left| \alpha \sum_{j=1}^{n-1} (-1)^{\omega_j} cA^j be_{c(n-j)}^\gamma \right|$. For a given combination of $\{\omega_1, \omega_2, \ldots, \omega_{n-1}\}$, we can obtain three scenarios of the convergence limits by comparing M_{n-1}^ω and M^*, similar to the discussions for the case of $t = 2$ in Section III-B. Then, we obtain the following theorem.

Theorem 4: Consider the error dynamics (3). The error $e_k(t)$ converges to a limit cycle, determined as follows. For any $t > 1$, suppose the limit cycle of $e_k(i)$ is $\pm e_{ci}$ for $1 \le i \le t-1$. Define a nonlinear equation

$$-x = x - \alpha cb|x|^\gamma \text{sgn}(x) - M_{t-1}^\omega \tag{22}$$

where $M_{t-1}^\omega \triangleq \left| \alpha \sum_{j=1}^{t-1} (-1)^{\omega_j} cA^j be_{c(t-j)}^\gamma \right|$ for any given combination of $\{\omega_1, \omega_2, \ldots, \omega_{t-1}\}$. Then, the limit for e_{ct} are as follows.

a) If $M_{t-1}^\omega > M^*$, (22) has one root a_{t1} and $e_{ct} = |a_{t1}|$;

b) If $M_{t-1}^\omega = M^*$, (22) has two roots a_{t2} and b_{t2}, we obtain $e_{ct} = |a_{t2}|$ or $e_{ct} = |b_{t2}|$; and

c) If $M_{t-1}^\omega < M^*$, (22) has three roots a_{t3}, b_{t3} and c_{t3}, satisfying $a_{t3} < b_{t3} < c_{t3}$, we obtain $e_{ct} = |a_{t3}|$ or $e_{ct} = |c_{t3}|$.

Once the initial tracking error $e_0(t)$ is determined, the error $e_k(t)$ converges to a limit cycle, i.e., $\lim_{k \to \infty} e_k(t) = \pm e_{ct}$.

Remark 7: It is worth noting that initial values of $e_0(t)$, $t = 1, 2, \ldots$, exists such that $e_k(t) = 0$ after a finite number of iterations. Therefore, the tracking error is either equal to zero after a finite number of iterations or convergent to a limit cycle of period two. However, the measure of a set of initial values ensuring $e_k(t) = 0$ after a finite number of iterations is zero in the corresponding space.

Remark 8: For the proposed update rule (2), if we let $\gamma = 1$, it becomes the conventional P-type update rule. For a P-type update rule, the learning gain α is usually required to satisfy

$0 < \alpha cb < 2$ to ensure convergence. Thus, both the sign and bound of cb are necessary for the selection of α. In (2), only the sign is required; in other words, less information is required compared to the P-type update rule. Accordingly, zero-error tracking performance is difficult to realize by the fractional power update rule, but can be tuned by the parameter selection. That is, by tuning the parameters, the fixed value of the limiting cycle can be as close to zero as possible. However, any parameter selection cannot lead to convergence to a unique limit due to fractional power innovation. Furthermore, for the P-type update rule with $\gamma = 1$ and $0 < \alpha cb < 2$, the root of (22) is $x = 0$ only for any time instant and therefore, zero-error tracking performance is ensured. In other words, the P-type update rule can be regarded as a special case of the proposed rule (2).

Remark 9: We note that the fractional power update rule enhances the convergence performance by automatically increasing the update intensity driven by tracking errors. In particular, the convergence rate is increased when the tracking error is small. Therefore, for practical applications, we can first apply the P-type update rule to guarantee a fast reduction of the tracking error and then switch to the fractional power update rule to further enhance the performance.

IV. NUMERICAL SIMULATIONS

We apply the fractional power update rule to control of a permanent magnet linear motor (PMLM) model [29], which is described by (1) with the following system matrices:

$$A = \begin{bmatrix} 1 & 0.01 \\ 0 & -0.125 \end{bmatrix}, \quad b = \begin{bmatrix} 0 \\ 2 \end{bmatrix}, \quad c = \begin{bmatrix} 0 & 1 \end{bmatrix}.$$

The iteration length is set to $n = 20$. For each iteration, the initial state and input are set to 0, i.e., $x_k(0) = 0$, $\forall k$, and $u_0(t) = 0$, $\forall t$.

The desired output is a group of numbers $\{y_d(t), 1 \le t \le n\}$, randomly selected within $[0, 10]$ prior to the simulation. We apply the following fractional power update rule (2) with parameters $\alpha = 1$ and $\gamma = 0.5$. The algorithm is run for 50 iterations in each experimental trial.

A. Convergent Limit Cycle

In this subsection, we verify the validity of the convergent limit cycles. To this end, we first calculate the limits according to Theorem 4 for $t = 1, 2, 3$ as an illustration, and then run 100 independent trials to examine the actual limits. After that, we present the error profiles of all time instants along the iteration axis for an arbitrary trial.

First, we calculate the theoretical limits.

1) For $t = 1$, by Theorem 4, we have $e_{c1} = (\frac{\alpha cb}{2})^{\frac{1}{1-\gamma}} = 1$;

2) For $t = 2$, we have $|\alpha cAbe_{c1}^\gamma| = 0.25$, which is less than $M^* = 2(\frac{1}{\gamma} - 1)(\frac{\gamma \alpha cb}{2})^{\frac{1}{1-\gamma}} = 0.5$. By Theorem 4, e_{c2} has two possible values, which are solutions of the equation $x = -x + \alpha cb|x|^\gamma \text{sgn}(x) - |\alpha cAbe_{c1}^\gamma|$. By substituting parameters in this equation, it transforms into a pair of equations: $x = -x + 2x^{\frac{1}{2}} - 0.25$ for $x \ge 0$ and $x = -x - 2(-x)^{\frac{1}{2}} - 0.25$ for $x < 0$. From the former equation, we obtain $x_1 = 0.0214$ and $x_2 = 0.7286$, whereas from the latter one, we obtain $x_1' = -1.2374$.

According to Theorem 4, we obtain $a_{13} = -1.2374$, $b_{13} = 0.0214$ and $c_{13} = 0.7286$. Thus, the limit cycle is ± 0.7286 or ± 1.2374; that is, e_{c2} is equal to either 0.7286 or 1.2374;

3) For $t = 3$, we note that $|\alpha cAbe_{c2}^{\gamma} + \alpha cA^2 be_{c1}^{\gamma}| < M^*$ and $|\alpha cAbe_{c2}^{\gamma} - \alpha cA^2 be_{c1}^{\gamma}| < M^*$ for any possible value of e_{1c} and e_{2c}. To calculate the limit, consider the equation $x = -x + \alpha cb|x|^{\gamma} \text{sgn}(x) - M_2$ where $M_2 = |\alpha cAbe_{2c}^{\gamma} \pm \alpha cA^2 be_{1c}^{\gamma}|$. Regarding all possible combinations of e_{c1} and e_{c2}, we list the corresponding values of M_2 in Table I. Then, the possible limits are calculated from the following groups of equations:

$$(A)\begin{cases} x = -x + 2x^{\frac{1}{2}} - 0.1821 & (x \geq 0) \\ x = -x - 2(-x)^{\frac{1}{2}} - 0.1821 & (x < 0) \end{cases}$$

$$(B)\begin{cases} x = -x + 2x^{\frac{1}{2}} - 0.2446 & (x \geq 0) \\ x = -x - 2(-x)^{\frac{1}{2}} - 0.2446 & (x < 0) \end{cases}$$

$$(C)\begin{cases} x = -x + 2x^{\frac{1}{2}} - 0.2468 & (x \geq 0) \\ x = -x - 2(-x)^{\frac{1}{2}} - 0.2468 & (x < 0) \end{cases}$$

$$(D)\begin{cases} x = -x + 2x^{\frac{1}{2}} - 0.3093 & (x \geq 0) \\ x = -x - 2(-x)^{\frac{1}{2}} - 0.3093 & (x < 0). \end{cases}$$

TABLE I
POSSIBLE VALUES OF M_2 FOR THE CASE $t = 3$

e_{1c}	e_{2c}	M_2	e_{1c}	e_{2c}	M_2
1	0.7286	0.1821	−1	0.7286	0.2446
1	−0.7286	0.2446	−1	−0.7286	0.1821
1	1.2374	0.2468	−1	1.2374	0.3093
1	−1.2374	0.3093	−1	−1.2374	0.2468

The solutions of these equations are collected, rearranged, and presented in Table II, which lists all possible limits of error iteration (3) for $t = 3$.

TABLE II
POSSIBLE LIMITS FOR THE CASE $t = 3$

	A	B	C	D
c_3	0.8076	0.7351	0.7324	0.6541
a_3	−1.1751	−1.2325	−1.2345	−1.2908

To verify the theoretical limits, we perform the simulation for 100 independent trials with the initial error $e_0(t)$ varying from 0 to 10 randomly for each trial. Then, we collect the errors at the 50th iteration $e_{50}(t)$ for $t = 1, 2, 3$, respectively. The calculated values and simulation results are depicted in Fig. 4, denoted by dashed lines and circles, respectively. We made the following observations.

1) Fig. 4(a) shows the absolute values of $e_{50}(1)$ for 100 independent trials. The absolute value $|e_{50}(1)|$ is equal to 1 whenever the initial error does not belong to $\mathcal{A}$. Three convergent values are equal to zero because their initial errors belong to $\mathcal{A}$;

2) Fig. 4(b) shows the absolute values of $e_{50}(2)$ for 100 independent trials. Here, the possible limits have two values. Most of the outcomes $|e_{50}(2)|$ fall on the lines of $y = 1.2374$
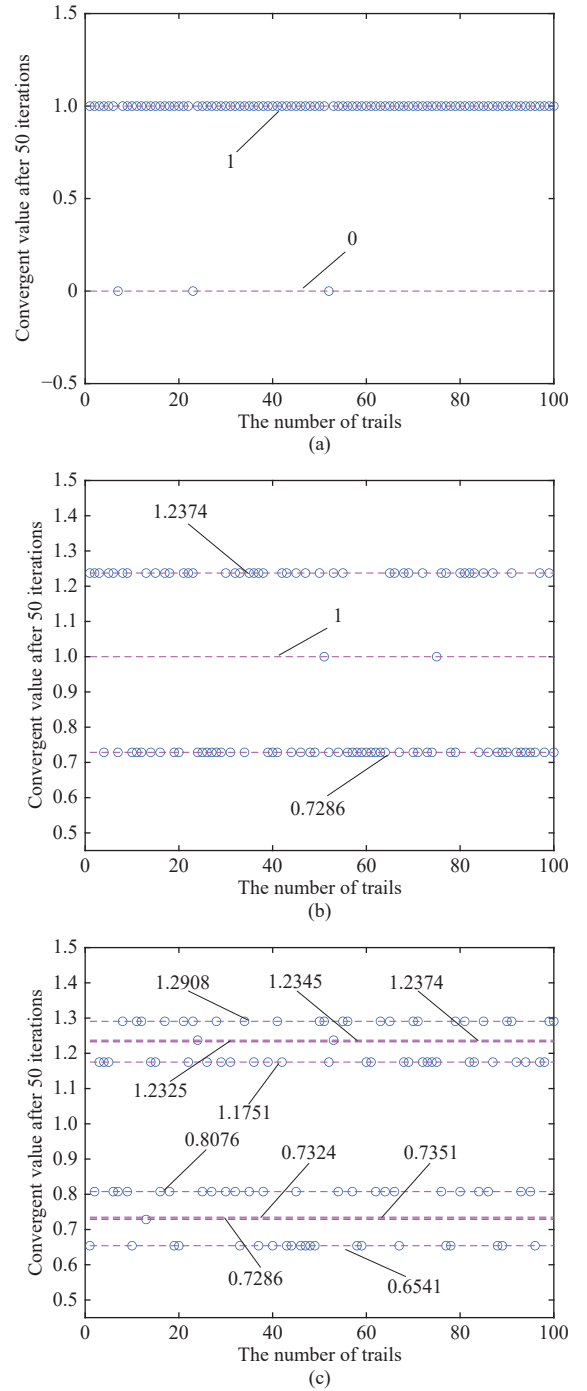

Fig. 4. Illustrations of (a) $|e_{50}(1)|$, (b) $|e_{50}(2)|$, and (c) $|e_{50}(3)|$ for 100 trials with initial tracking errors varying from 0 to 10 randomly.

and $y = 0.7286$. Moreover, several limits are equal to 1; this is because the corresponding initial errors for $t = 1$ belong to $\mathcal{A}$, and then, the evolution of the tracking error for $t = 2$ becomes the same as that for $t = 1$;

3) Fig. 4(c) shows the absolute value of $e_{50}(3)$ for 100 independent trials. The first interesting observation is that, although we have eight possible limits of e_{c3}, the outcomes of $|e_{50}(3)|$ mainly fall in four cases of the eight limits. The inherent reason for this is that αcb and αcAb have the same sign; otherwise, if αcb and αcAb have opposite signs, the outcomes would have fallen on the set of the other four cases.

Besides, some sparse values are equal to either 1.2374 or 0.7286, which is due to the degeneration of error dynamics when $e_0(1)$ belongs to $\mathcal{A}$.

In short, the numerical outcomes of the limit values in Fig. 4 are consistent with the theoretical result given by Theorem 4. We should mention that Fig. 4 is derived from different executions of the scheme to exhibit more possible situations. Moreover, the number of possible limits increases as the time label number increases.

We consider one simulation trial with ten iterations. Fig. 5 shows the convergence process of both tracking errors $e_k(t)$ and absolute tracking errors $|e_k(t)|$ for all time instants along the iteration axis. Each line corresponds to an iteration evolution for one time instant. Each error profile fluctuates between two opposite values after a few iterations in Fig. 5(a), indicating that the proposed learning rule yields asymptotic convergence of the tracking error to a limit cycle. Besides, Fig. 5(b) shows the convergence of the absolute tracking error.
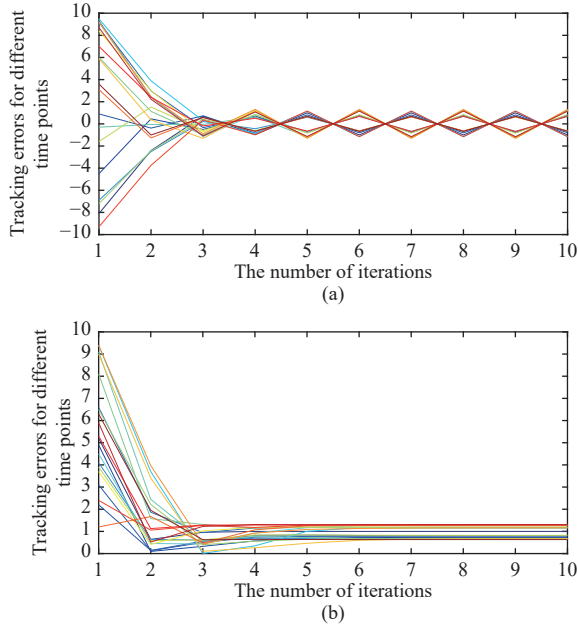

Fig. 5. Illustration of $e_k(t)$ (top) and $|e_k(t)|$ (bottom) with initial tracking errors varying from 0 to 10 randomly.

B. Tracking Precision

In this subsection, we examine the relationship between the tracking precision of the proposed scheme and the adjustable parameters. We compare the performance of the proposed rule with the P-type update rule: $u_{k+1}(t) = u_k(t) + \alpha e_k(t+1)$. To reflect the findings, we illustrate the tracking precision for the case of $t = 20$.

We first consider the effect of the learning gain α. To ensure convergence of both the proposed scheme and the P-type update rule, we let $0 < \alpha cb < 1$, implying $0 < \alpha < \frac{1}{2}$. Four cases are considered: $\alpha = 0.15, 0.25, 0.35$, and 0.45. The fractional power is set to $\gamma = 0.5$. The profiles of the maximum absolute tracking error $e_k(t)$ along the iteration axis are shown in Fig. 6. The figure shows that the convergence speed for the fractional power update rule is nearly the same for different
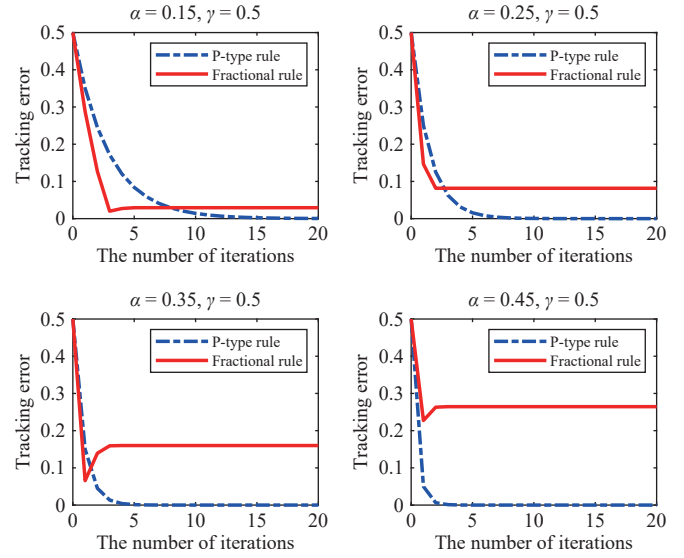

Fig. 6. Tracking precision for fractional power and P-type update rules with varying learning gains.

learning gains, requiring approximately two or three iterations to achieve the limit. In contrast, the learning gain has a significant influence on the convergence speed of the P-type update rule. A larger learning gain corresponds to a quick convergence for the P-type update rule. Furthermore, for a small learning gain, the fractional power update rule exhibits faster convergence than the P-type update rule. This is because the fractional power γ rather than the learning gain dominates the convergence rate for the fractional power update rule, differing from the P-type update rule where the convergence rate is determined by contraction factor $|1 - \alpha cb|$. In addition, tracking precision is distinct from the change in the learning gain for the fractional power update rule. Generally, a smaller learning gain corresponds to a smaller tracking error.

Then, we verify the effect of parameters γ while fixing the learning gain to be $\alpha = 0.15$. Four cases are considered, $\gamma = 0.125, 0.5, 0.75$, and 0.9. The profiles of the maximum absolute tracking error along the iteration axis are depicted in Fig. 7. A primary observation arises where as γ approaches one, the final tracking error is significantly reduced, indicating better tracking performance. However, the improvement of the final tracking precision comes at a certain cost in terms of convergence speed; that is, the convergence speed reduces as γ approaches one. Furthermore, the tracking performance of the proposed update rule approximates that of the P-type update rule as γ approaches one. In any case, the fractional power update rule exhibits a faster convergence rate for high precision error tracking. This demonstrates connections between the fractional power and P-type update rules. These observations are consistent with the theoretical results in Section III.

We should point out that the proposed fractional power update rule exhibits fine robustness against random noise. In other words, for system (1) with process and measurement noise, the tracking error generated by the proposed update rule would converge to a bounded zone, which is similar to that for the P-type update rule. However, it is difficult to present a
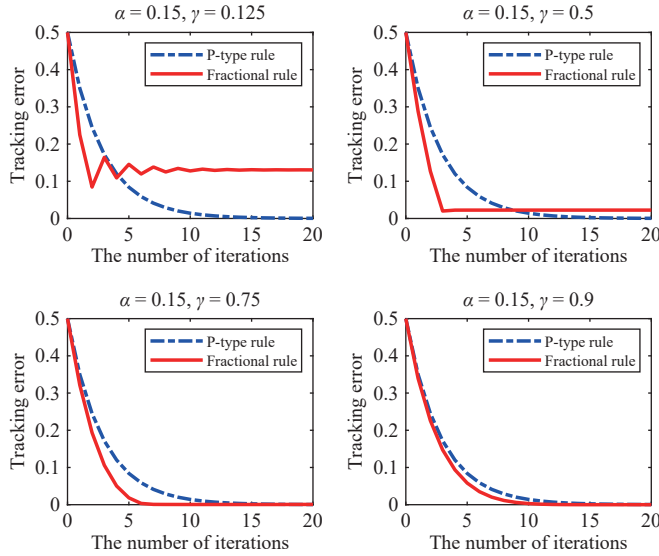
Fig. 7. Tracking precision for fractional power update rule with different fractional powers.

quantitative depiction of the influence of random noise on tracking performance, which is left for future research.

V. CONCLUSIONS

In this study, a fractional power update rule has been proposed for ILC of SISO linear systems, yielding an innovative design paradigm beyond the traditional P-type update rule. It has been shown that the nonlinear update control in essence can improve learning ability, similar to FTC and TSMC. A systematic convergence analysis has been done for the proposed fractional power update rule. The convergence has been proved inductively along the time axis by investigating the evolutionary behaviors of the error dynamics. The limit cycles for each time instant have been characterized recursively using a nonlinear equation, along with limit combinations of the previous time instants. Numerical simulations have demonstrated the effectiveness and advantages of the proposed fractional power update rule.

APPENDIX

Proof of Lemma 2: Define $V(u) \triangleq \|u - v\|$. We have $\Delta V(u) = V(f(u)) - V(u) = \|f(u) - v\| - \|u - v\| < 0$. Thus, $V(u)$ is a strict Lyapunov function. By Lemma 1, v is asymptotically stable in B. ∎

Proof of Lemma 3: Suppose $|f'(x^*)| = \rho > 1$. By the continuity of f', there exists a neighborhood $U^o(x^*)$ of x^* such that for every $x \in U^o(x^*)$, $|f'(x)| > 1$. Thus, if $x_k \in U^o(x^*)$, we have $|x_{k+1} - x^*| = |f(x_k) - f(x^*)| = |f'(\xi_k)||x_k - x^*| > |x_k - x^*|$, where $\xi_k \in (x_k, x^*)$ or (x^*, x_k). Then, $|x_{k+1} - x^*|$ will be larger than $|x_k - x^*|$ if $x_k \neq x^*$, and the lemma is proven. ∎

Proof of Lemma 4: Define $P_k = X(k) - X^*$ and $\mathbf{1} = [1, 1, \ldots, 1]^T$. For $x_1(k+1) = f_1(x_1(k), x_2(k), \ldots, x_n(k))$, we obtain

$$x_1(k+1) = f_1(X^*) + \nabla f_1(X^*)^T P_k$$
$$+ \frac{1}{2!} P_k^T \nabla^2 f_1((1-\sigma)X^* + \sigma X(k)) P_k$$
$$= x_1^* + \nabla f_1(X^*)^T P_k + o(\|P_k\|).$$

Hence, $P_{k+1} = \nabla F(X^*) P_k + o(\|P_k\|)\mathbf{1}$. Then, there exists a ball $B(X^*, r)$ such that when $P_k \in B(X^*, r)$, we have

$$\|P_{k+1}\| \leq \|\nabla F(X^*) P_k\| + \|o(\|P_k\|)\mathbf{1}\|$$
$$\leq \left(\|\nabla F(X^*)\| + \frac{o(\|P_k\|)}{\|P_k\|}\right)\|P_k\|$$
$$< \vartheta\|P_k\|$$

where $0 < \vartheta < 1$ is a constant. Hence, $\lim_{k\to\infty} \|P_k\| = 0$. Therefore, for every $X(0) = X_0$ in $B(x^*, r)$ as the initial value of (4), we have $\lim_{k\to\infty} X(k) = X^*$. ∎

REFERENCES

[1] D. A. Bristow, M. Tharayil, and A. G. Alleyne, "A survey of iterative learning control: A learning-based method for high performance tracking control," *IEEE Control Systems Magazine*, vol. 26, no. 3, pp. 96–114, 2006.

[2] D. Meng and J. Zhang, "Robust optimization-based iterative learning control for nonlinear systems with nonrepetitive uncertainties," *IEEE/CAA J. Autom. Sinica*, vol. 8, no. 5, pp. 1001–1014, 2021.

[3] Y. Hui, R. Chi, B. Huang, and Z. Hou, "Extended state observer-based data-driven iterative learning control for permanent magnet linear motor with initial shifts and disturbances," *IEEE Trans. Systems, Man, and Cybernetics: Systems*, vol. 51, no. 3, pp. 1881–1891, 2021.

[4] A. A. Armstrong, A. J. Wagoner Johnson, and A. G. Alleyne, "An improved approach to iterative learning control for uncertain systems," *IEEE Trans. Control Systems Technology*, vol. 29, no. 2, pp. 546–555, 2021.

[5] D. Shen, "Practical learning-tracking framework under unknown nonrepetitive channel randomness," *IEEE Trans. Automatic Control*, pp. 1–16, 2022.

[6] A. Deutschmann-Olek, G. Stadler, and A. Kugi, "Stochastic iterative learning control for lumped- and distributed-parameter systems: A wiener-filtering approach," *IEEE Trans. Automatic Control*, vol. 66, no. 8, pp. 3856–3862, 2021.

[7] Z. Wang, R. Zhou, C. Hu, and Y. Zhu, "Online iterative learning compensation method based on model prediction for trajectory tracking control systems," *IEEE Trans. Industrial Informatics*, vol. 18, no. 1, pp. 415–425, 2022.

[8] C. Hua, Y. Qiu, and X. Guan, "Event-triggered iterative learning containment control of model-free multiagent systems," *IEEE Trans. Systems, Man, and Cybernetics: Systems*, vol. 51, no. 12, pp. 7719–7726, 2021.

[9] F. H. Kong and I. R. Manchester, "Contraction analysis of nonlinear noncausal iterative learning control," *Systems & Control Letters*, vol. 136, p. 104599, 2020.

[10] Q. Yu and Z. Hou, "Adaptive fuzzy iterative learning control for high-speed trains with both randomly varying operation lengths and system constraints," *IEEE Trans. Fuzzy Systems*, vol. 29, no. 8, pp. 2408–2418, 2021.

[11] X. Bu and Z. Hou, "Adaptive iterative learning control for linear systems with binary-valued observations," *IEEE Trans. Neural Networks and Learning Systems*, vol. 29, no. 1, pp. 232–237, 2018.

[12] X. Jin, "Adaptive iterative learning control for high-order nonlinear multi-agent systems consensus tracking," *Systems & Control Letters*, vol. 89, pp. 16–23, 2016.

[13] W. Xiong, L. Xu, T. Huang, X. Yu, and Y. Liu, "Finite-iteration tracking of singular coupled systems based on learning control with packet losses," *IEEE Trans. Systems, Man, and Cybernetics: Systems*, vol. 50, no. 1, pp. 245–255, 2020.

[14] W. Xiong, D. W. Ho, and S. Wen, "A periodic iterative learning scheme for finite-iteration tracking of discrete networks based on flexray communication protocol," *Information Sciences*, vol. 548, pp. 344–356, 2021.

[15] X. Cheng, H. Jiang, D. Shen, and X. Yu, "A novel adaptive gain

strategy for stochastic learning control," *IEEE Trans. Cybernetics*, pp. 1–12, 2022.

[16] V. T. Haimo, "Finite time controllers," *SIAM Journal on Control and Optimization*, vol. 24, no. 4, pp. 760–770, 1986.

[17] S. P. Bhat and D. S. Bernstein, "Finite-time stability of continuous autonomous systems," *SIAM Journal on Control and Optimization*, vol. 38, no. 3, pp. 751–766, 2000.

[18] W. M. Haddad and A. L'Afflitto, "Finite-time stabilization and optimal feedback control," *IEEE Trans. Automatic Control*, vol. 61, no. 4, pp. 1069–1074, 2016.

[19] S. Yu, X. Yu, B. Shirinzadeh, and Z. Man, "Continuous finite-time control for robotic manipulators with terminal sliding mode," *Automatica*, vol. 41, no. 11, pp. 1957–1964, 2005.

[20] X. Yu, J.-X. Xu, Y. Hong, and S. Yu, "Analysis of a class of discrete-time systems with power rule," *Automatica*, vol. 43, no. 3, pp. 562–566, 2007.

[21] H. Hou, X. Yu, L. Xu, K. Rsetam, and Z. Cao, "Finite-time continuous terminal sliding mode control of servo motor systems," *IEEE Trans. Industrial Electronics*, vol. 67, no. 7, pp. 5647–5656, 2020.

[22] F. Wu, C. Li, and J. Lian, "Finite-time stability of switched nonlinear systems with state jumps: A dwell-time method," *IEEE Trans. Systems, Man, and Cybernetics: Systems*, vol. 52, no. 10, pp. 6061–6072, 2022.

[23] F. Tatari, H. Modares, C. Panayiotou, and M. Polycarpou, "Finite-time distributed identification for nonlinear interconnected systems," *IEEE/CAA J. Autom. Sinica*, vol. 9, no. 7, pp. 1188–1199, 2022.

[24] Y. Liu, H. Li, R. Lu, Z. Zuo, and X. Li, "An overview of finite/fixed-time control and its application in engineering systems," *IEEE/CAA J. Autom. Sinica*, vol. 9, no. 12, pp. 2106–2120, 2022.

[25] G. Sun, Z. Ma, and J. Yu, "Discrete-time fractional order terminal sliding mode tracking control for linear motor," *IEEE Trans. Industrial Electronics*, vol. 65, no. 4, pp. 3386–3394, 2018.

[26] F. Li, Z. Wu, C. Yang, Y. Shi, T. Huang, and W. Gui, "A novel learning-based asynchronous sliding mode control for discrete-time semi-Markov jump systems," *Automatica*, vol. 143, p. 110428, 2022.

[27] S. Kuang, D. Dong, and I. R. Petersen, "Rapid Lyapunov control of finite-dimensional quantum systems," *Automatica*, vol. 81, pp. 164–175, 2017.

[28] P. Ioannou and B. Fidan, *Adaptive Control Tutorial*. SIAM, 2006.

[29] W. Zhou, M. Yu, and D. Huang, "A high-order internal model based iterative learning control scheme for discrete linear time-varying systems," *Int. Journal of Automation and Computing*, vol. 12, no. 3, pp. 330–336, 2015.
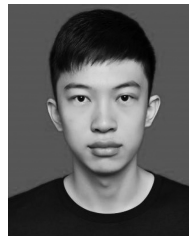
Zihan Li received the B.S. degree in mathematics from Hunan University in 2021. He is currently working toward the master degree with the School of Mathematics, Renmin University of China. His research interests include learning control and parameter estimation.

Dong Shen (Senior Member, IEEE) received the B.S. and Ph.D. degrees in mathematics from Shandong University, and the Academy of Mathematics and Systems Science, Chinese Academy of Sciences (CAS), in 2005 and 2010, respectively. From 2010 to 2012, he was a Post-Doctoral Fellow with the Institute of Automation, CAS. From 2012 to 2019, he was with the Beijing University of Chemical Technology. From 2016.02 to 2017.02, he was a Visiting Scholar at National University of Singapore, Singapore. From 2019.07 to 2019.08, he was a Visiting Research Fellow at RMIT University, Australia. Since 2020, he has been a Professor with the School of Mathematics, Renmin University of China. His research interests include iterative learning control, stochastic optimization, and distributed artificial intelligence. He is currently serving on the Editorial Board of *International Journal of Robust and Nonlinear Control* and *IET Cyber-Systems and Robotics*, and Early Career Advisory Board of *IEEE/CAA Journal of Automatica Sinica*.

Xinghuo Yu (Fellow, IEEE) received B.Eng. and M.Eng. degrees in electrical and electronic engineering from the University of Science and Technology of China, in 1982 and 1984, and Ph.D. degree in control science and engineering from Southeast University, in 1988, respectively.

He is a Distinguished Professor and a Vice-Chancellor's Professorial Fellow at Royal Melbourne Institute of Technology (RMIT University), Australia. He was the President of IEEE Industrial Electronics Society in 2018 and 2019. His research interests include control systems, complex and intelligent systems, and future energy systems. He served as an Associate Editor of *IEEE Transactions on Automatic Control*, *IEEE Transactions on Circuits and Systems I: Regular Papers*, *IEEE Transactions on Industrial Electronics* and *IEEE Transactions on Industrial Informatics*. He received a number of awards and honors for his contributions, including 2013 Dr.-Ing. Eugene Mittelmann Achievement Award of IEEE Industrial Electronics Society, and 2018 M. A. Sargent Medal from Engineers Australia. He is an Honorary Fellow of Engineers Australia.